In-beam γ-ray spectroscopy of $^{43-46}$Cl

S. R. Stroberg,[1,2] A. Gade,[1,2] T. Baugher,[1,2] D. Bazin,[1] B. A. Brown,[1,2] J. M. Cook,[1,2,*] T. Glasmacher,[1,2] G. F. Grinyer,[1,†] S. McDaniel,[1,2] A. Ratkiewicz,[1,2] and D. Weisshaar[1]

[1]*National Superconducting Cyclotron Laboratory, Michigan State University, East Lansing, Michigan 48824, USA*

[2]*Department of Physics and Astronomy, Michigan State University, East Lansing, Michigan 48824, USA*

(Received 15 June 2012; revised manuscript received 3 August 2012; published 31 August 2012)

The low-energy nuclear structure of the neutron-rich $^{43-46}$Cl isotopes is studied via in-beam γ-ray spectroscopy following the fragmentation of ^{48}K projectiles on a ^{9}Be target at intermediate beam energies. $\gamma\gamma$ coincidence information was used to construct level schemes for these neutron-rich nuclei. For the $N = 28$ nucleus ^{45}Cl, the lifetime of the first excited state at 130 keV was extracted via γ-ray line shape analysis, yielding an $M1$ strength an order of magnitude greater than that predicted by theory. The experimental data is compared to the results of large-scale shell-model calculations with effective interactions in the sd-pf model space.

DOI: 10.1103/PhysRevC.86.024321 PACS number(s): 23.20.Lv, 29.30.Kv, 23.20.En, 21.60.Cs

I. INTRODUCTION

With rare-isotope beam facilities in operation around the world, it has become clear that the nuclear shell model's "magic numbers" or shell closures—ubiquitous near the valley of stability—can break down at large proton-neutron asymmetry [1–3]. The magic number 28 is of particular interest because it is the lowest number—and thus the most readily accessible with experiments and the most tractable in shell-model calculations—whose emergence requires a strong spin-orbit interaction. Therefore, in addition to the phenomenon of shell evolution in the exotic regime, an understanding of the breakdown of the $N = 28$ shell closure far from stability can give insight into the isospin dependence of the spin-orbit interaction.

In recent years, experiments have shown that the $N = 28$ isotones ^{44}S ($Z = 16$) and ^{42}Si ($Z = 14$) are collective [4,5] with evidence for shape and configuration coexistence [6,7], signaling the breakdown of the neutron shell closure as protons are removed from the sd shell [4,5]. Measurements of excited states in the odd-Z neighbors potassium, chlorine, and phosphorus ($Z = 19, 17, 15$) have indicated a near-degeneracy of the $d_{3/2}$ and $s_{1/2}$ proton orbitals approaching $N = 28$ [8,9]. Both of these trends can be qualitatively explained by the monopole parts of the tensor force [10], which is attractive between the proton $d_{3/2}$ and neutron $f_{7/2}$ orbitals. These effects lead to enhanced quadrupole correlations across both the $Z = 14$ and $N = 28$ gaps, making ^{42}Si the most collective in the region [5].

A consistent theoretical description of nuclei in this region of the nuclear chart has remained a challenge, with the most successful shell-model effective interaction, SDPF-U [11], divided into two parts, one valid for for $Z > 14$ and one optimized for $Z \leqslant 14$. A new effective interaction based on the extended pairing quadrupole-quadrupole force with inclusion of a monopole term (EPQQM) was proposed recently [12] with the aim to provide a unified description of neutron-rich nuclei in the sd-fp shell. In order to benchmark emerging and existing theoretical descriptions of this interesting region, we have used in-beam γ-ray spectroscopy with $\gamma\gamma$ coincidence measurements following the fragmentation of a ^{48}K projectile beam to investigate the low-energy structure of $^{43-46}$Cl. For the $N = 28$ nucleus ^{45}Cl, the lifetime of its first excited state could be determined from the line shape of the 130 keV γ-ray transition. Previous knowledge on ^{43}Cl and ^{45}Cl stems from in-beam γ-ray spectroscopy following fragmentation reactions [8,13] and intermediate-energy Coulomb excitation [14]. The single-particle structure of ^{44}Cl was studied before via one-neutron knockout from ^{45}Cl [15] and with a ground-state g-factor measurement [16]. No previous spectroscopic data exist on ^{46}Cl.

II. EXPERIMENT

The experiment was performed at the Coupled Cyclotron Facility at the National Superconducting Cyclotron Laboratory at Michigan State University. A ^{48}K secondary beam was produced by nucleon exchange induced by a 140 MeV/u ^{48}Ca primary beam interacting with a 740 mg/cm^2 ^{9}Be production target, as described in Ref. [17]. The beam was purified in the A1900 fragment separator [18] with a 390 mg/cm^2 Al wedge degrader. The ^{48}K beam was then transmitted to the experimental setup with the momentum acceptance, $\Delta p/p$, restricted to 0.5% and impinged at a rate of approximately 2×10^5 pps upon a 376 mg/cm^2 ^{9}Be foil at the target position of the S800 spectrograph [19] with a midtarget energy of 85 MeV/u. The emerging projectile-like reaction products were identified event-by-event using the detectors in the focal plane of the S800 spectrograph in conjunction with plastic scintillators in the beam line for time-of-flight information. Figure 1 shows the particle identification spectrum that uses the energy loss measured with the S800 ionization chamber and the ion's flight times taken between two plastic scintillators (corrected for each ion's momentum and angle).

The reaction target was surrounded by the Segmented Germanium Array (SeGA) [20], an array of 32-fold segmented

*Present address: Los Alamos National Laboratory, Los Alamos, NM 87545, USA.

†Present Address: Grand Accélérateur National d'Ions Lourds (GANIL), CEA/DSM-CNRS/IN2P3, Blvd Henri Becquerel, 14076 Caen, France.

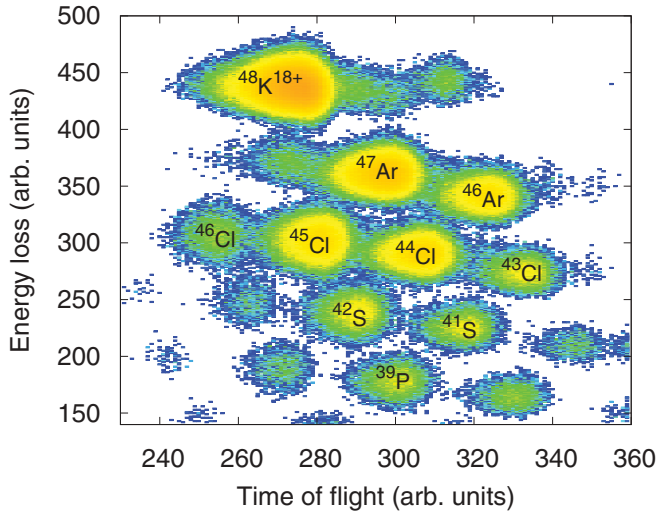

FIG. 1. (Color online) Particle identification spectrum for the reaction residues produced in ^{48}K(^{9}Be,X)Y. Energy loss was measured in the ionization chamber of the S800 focal plane. The time-of-flight was taken between plastic scintillators in the beam line and in the back of the S800 focal plane. The Cl isotopes of interest can be unambiguously identified.

HPGe detectors. The SeGA detectors were arranged in two rings, with seven detectors at 37° and ten at 90° with respect to the beam line. The location of the detector segment that registered the largest energy deposition was used to compute the γ-ray emission angle that entered the Doppler reconstruction needed for the γ rays emitted by the reaction products in flight. Doppler-corrected γ-ray spectra detected in coincidence with the respective chlorine isotopes are shown in Figs. 2, 5, and 9.

In the offline analysis, all γ rays detected within a 600-ns time window were considered to be coincident and stored in a two-dimensional coincidence matrix. Coincidences between individual γ rays, shown in Figs. 3, 6, and 11, were obtained by software gates on the full-energy peak in the coincidence matrix. Background was estimated from a gate on a featureless

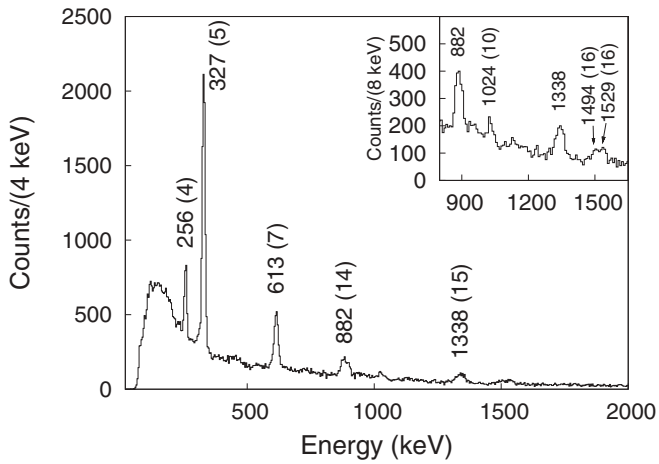

FIG. 2. Doppler-corrected γ-ray spectrum ($v/c = 0.408$) in coincidence with ^{43}Cl. The inset shows the peaks above 1 MeV in greater detail.

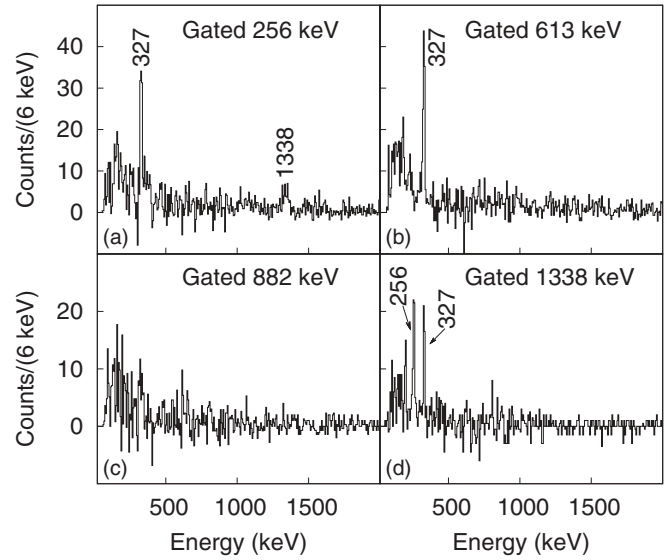

FIG. 3. Background-subtracted $\gamma\gamma$ coincidence spectra for ^{43}Cl.

section of the spectrum on the high-energy side of the peak. All coincidence spectra shown in this work are background subtracted.

An efficiency calibration of the SeGA setup was performed with standard γ-ray calibration source of known activity. The γ-ray detection efficiency entered the determination of the relative intensities of the γ-ray transitions, shown in Tables I, II, VI, and VII and was used in some cases to determine the ordering of coincident γ-rays in a coincidence cascade.

III. RESULTS AND DISCUSSION

In the following, we discuss our results for ^{43}Cl, ^{45}Cl, and ^{44,46}Cl separately. The measured data and the proposed level schemes are compared to large-scale shell-model calculations using the SDPF-U [11] and EPQQM [12] effective interactions for the sd-pf shell, with an empty proton fp shell, and a filled neutron sd shell. SDPF-U is an updated version of SDPF-NR [21], adjusted to better fit recent data on very neutron-rich nuclei. It is essentially split into two separate effective interactions, one for $Z \leqslant 14$ and one for $Z > 14$. In these calculations, we used the interaction with $Z > 14$. Extended pairing, quadrupole-quadrupole and monopole (EPQQM) is a recent effective interaction aimed at a unified description of neutron-rich nuclei in this region.

A. ^{43}Cl

Figure 2 shows the Doppler-reconstructed γ-ray spectrum taken in coincidence with ^{43}Cl reaction residues. Five γ-ray transitions are clearly present, at 256, 327, 613, 882, and 1338 keV. Additionally, there is a less intense peak visible at 1024 keV and a likely doublet at 1494 and 1529 keV (see Fig. 2 inset). All five of the strong peaks were observed previously in Ref. [8], and a peak at 1509(10) keV was reported in Ref. [13]. From the $\gamma\gamma$ coincidence data displayed in Fig. 3, we obtain the coincidence relations shown in

TABLE I. γ-Ray energies, efficiency-corrected relative intensities, and coincidences for ^{43}Cl.

E_γ [keV]	I_γ [%]	Coincident γ rays
256	18(1)	327, 1338
327	100(3)	256, 613
613	45(3)	327
882	30(3)	
1024	7(2)	
1338	22(3)	256, 327

Table I, resulting in our proposed level scheme in Fig. 4. Due to its intensity, the 327-keV transition is assumed to connect the first excited state and the ground state. There is a clear coincidence between the 327- and 613-keV transitions, as reported in Ref. [13]. We do not observe the coincidence of the 882-keV transition with either of those two transitions as proposed by Ref. [13]. Based on our data, the 882 keV transition is tentatively placed decaying directly to the ground state. The 256-, 327-, and 1338-keV transitions are seen in mutual coincidence, although the ordering of the 256 and 1338 keV transitions is difficult to discern from this data set alone because the efficiency-corrected intensities of the two transitions, listed in Table I, agree within the uncertainties. In Ref. [8], however, the intensity of the 256-keV γ-ray transition is significantly smaller than the intensity of the 1338-keV peak and, thus, together with the coincidence relation established here, the 256-keV transition is placed above the 1338-keV transition in the level scheme. The intensity equality observed here indicates that, unlike in the previous experiment that used a ^{46}Ar projectile beam [8], the intermediate state at 1665 keV in this cascade has a negligible direct population in the fragmentation of ^{48}K.

In Fig. 4, the proposed level scheme is compared to shell-model calculations. SDFP-U and EPQQM produce similar level schemes with a $1/2^+$ ground state, a $3/2^+$ first excited

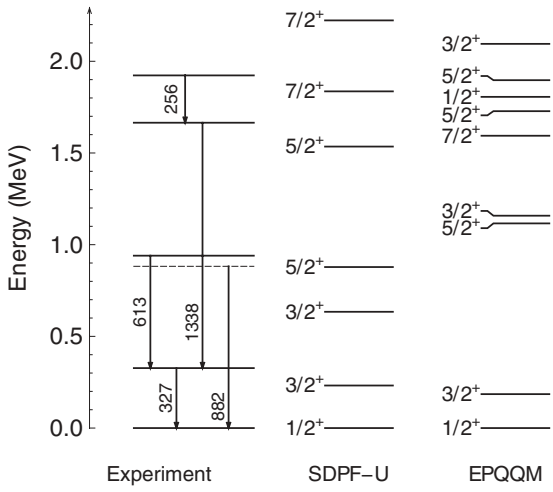

FIG. 4. Level scheme for ^{43}Cl from this work and shell-model calculations using the SDPF-U [11] and EPQQM [12] effective interactions. The dashed line in the experimental level scheme indicates a tentative level assignment.

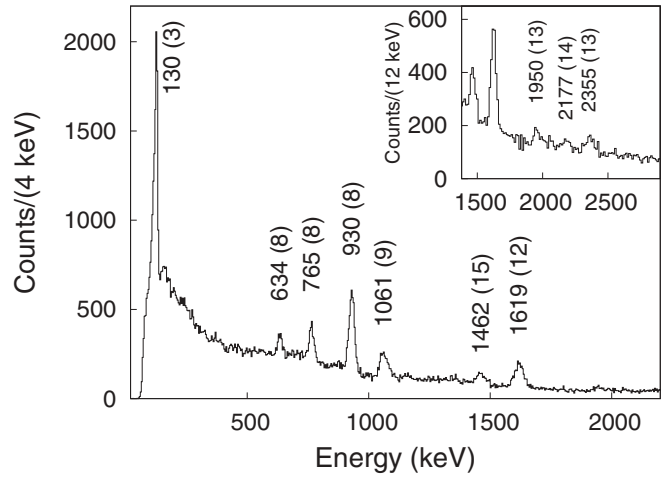

FIG. 5. Doppler-corrected γ-ray spectrum ($v/c = 0.393$) in coincidence with ^{45}Cl. The inset plot shows the peaks near 2 MeV in more detail.

state within 300 keV, and close-lying $3/2^+$ and $5/2^+$ higher-excited states. These two states are predicted to be nearly degenerate and slightly above 1 MeV by EPQQM, while SDPF-U calculates them at 630 and 880 keV, respectively. Above 1.5 MeV, SDPF-U predicts a $5/2^+$ state and two $7/2^+$ states, all separated by several hundred keV, while EPQQM predicts five closely spaced states with J^π values from $1/2^+$ to $7/2^+$ in the energy window of 1.5 to 2.2 MeV. Our level scheme agrees with the features calculated in the shell model with the ground and first excited states within 400 keV and two near-degenerate excited states around 1 MeV. Only two excited states, separated by about 300 keV, are observed above 1.5 MeV, more consistent with the SDPF-U calculation.

B. ^{45}Cl

The Doppler-reconstructed ^{45}Cl γ-ray spectrum is displayed in Fig. 5. Seven transitions are clearly visible at 130, 634, 765, 930, 1061, 1462, and 1619 keV. There are also indications of transitions at 1950, 2177, and 2355 keV, which could not be placed in the level scheme proposed here. The 930-keV transition was first observed in intermediate-energy Coulomb excitation [14], strongly suggesting that it de-excites a quadrupole collective state to the ground state. The 130-, 765-, 930-keV transitions were previously reported in Ref. [8] and the 930- and 1619-keV peaks in Ref. [13].

The $\gamma\gamma$ coincidence matrix gated on the 130 keV peak, which is taken as the decay of the first excited state in agreement with Ref. [8], reveals a clear coincidence with the 634-keV transition (Fig. 6). This, combined with intensity balance arguments, excludes the possibility of any of the more intense transitions feeding the first excited state. There is also evidence for a coincidence between the 1619- and 1061-keV peaks (Fig. 6). The 1061-keV transition is placed above the 1619-keV transition based on their relative intensities. From this information, we construct the level scheme shown in Fig. 7, consistent with the coincidence relations and intensities summarized in Table II.

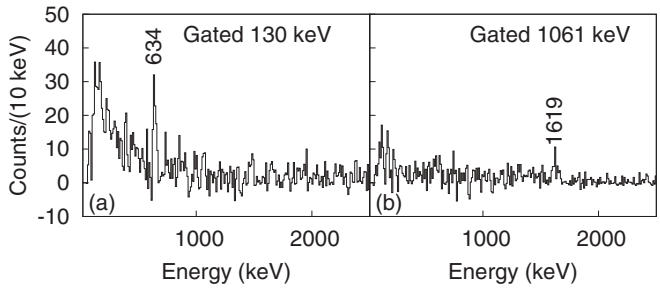

FIG. 6. Background-subtracted $\gamma\gamma$ coincidence spectra for ^{45}Cl. The reciprocal coincidences are also seen.

The peak shape of the 130-keV transition shows a pronounced asymmetry (Fig. 8). This low-energy tail of the peak indicates a lifetime effect of the order of several hundred picoseconds, as long-lived states decay on average behind the target while the Doppler reconstruction assumes a midtarget decay. This leads to an underestimation of the angle of emission and corresponding underestimation of the energy of the emitted γ ray in the rest frame of the projectile and consequently to a low-energy tail on the peak.

The measured peak shape was fit with response functions simulated with GEANT4 [22]. The best-fit lifetime was determined in a two-parameter χ^2 minimization of the peak energy and level lifetime for each ring of SeGA (see Fig. 8 for the best fit). In the simulation, the incoming beam energy was matched to the settings of magnetic dipoles before the target, and the width of the momentum distribution was taken from the slit setting of the A1900 and verified with settings where the beam passed through the target unreacted. For ^{45}Cl produced in the fragmentation of ^{48}K, the broadening of the ^{45}Cl distribution relative to the spread in momentum and angle of the incoming projectile beam were modeled with Gaussians to reproduce the scattering angle and

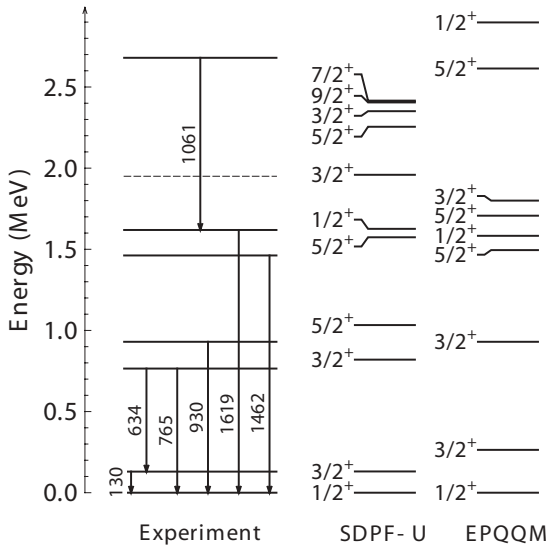

FIG. 7. Level scheme for ^{45}Cl from this work and shell-model calculations using the SDPF-U and EPQQM residual interactions. The dashed line in the experimental level scheme indicates the energy of the 1950-keV transition shown in the inset of Fig. 5.

TABLE II. γ-Ray energies, efficiency-corrected relative intensities, and coincidences for ^{45}Cl.

E_γ [keV]	I_γ [%]	Coincident γ rays
130	63(9)	634
634	15(2)	130
765	33(2)	
930	100(3)	
1061	41(3)	1619
1462	30(4)	
1619	73(5)	1061

parallel momentum distributions of ^{45}Cl measured in the S800 spectrograph. The energy threshold of the SeGA detectors was modeled as a hyperbolic tangent and fit to source data. Finally, a Doppler reconstruction identical to that used for the measured in-beam spectrum was applied. The shape of the background was constrained by fitting an inverse tangent plus an exponential to in-beam spectra in coincidence with ^{46,47}Ar or ^{42}S. These nuclei were chosen to provide the shape of the background because of their relatively high statistics and the absence of significant transitions in the relevant low-energy region. The two-parameter χ^2 minimization was performed separately for the forward and backward rings of SeGA, yielding an energy of 130.2(20) keV and the lifetimes indicated in Fig. 8. Taking into account statistical and systematic uncertainties, we obtain a lifetime for the first excited state of $\tau = 470(60)$ ps. The systematic uncertainties were estimated from variations in the inputs to the simulations and reflect their sensitivities. Assuming that at such a low excitation energy the transition is of pure $M1$ character, this lifetime corresponds to $B(M1\downarrow)_{\rm exp} = 0.055(7)\mu_N^2$.

For ^{45}Cl, SDPF-U is in outstanding agreement with the proposed experimental level scheme. However, there is a

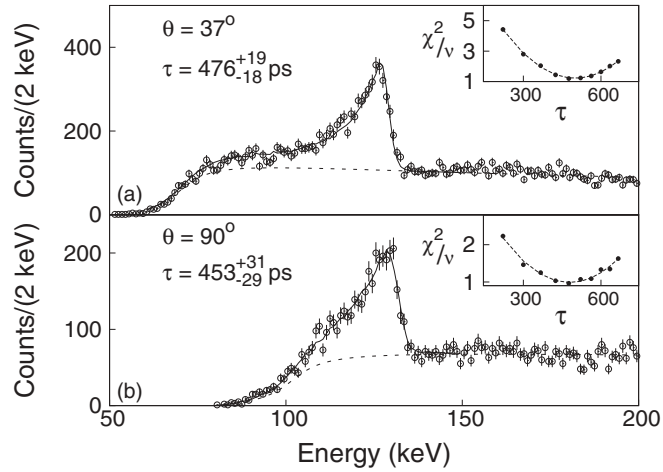

FIG. 8. 130-keV peak in ^{45}Cl detected in the forward ring (top panel) and backward ring (bottom panel) of SeGA, Doppler-reconstructed with $v/c = 0.393$. The spectra are fit with a GEANT4 simulation using the best-fit lifetime (solid line) on top of a fit to the measured background (dashed line). The insets show the reduced χ^2 minimization for the lifetime of the peak. Note that τ is shown with a log scale.

TABLE III. Results of a calculation using SDPF-U and the allowed $M1$ operator from Ref. [16]. S_p, P_n, etc. indicate reduced matrix elements of the given operator; P indicates the tensor operator of Eq. (1); while the subscripts indicate the proton or neutron component. $M1_{L+S}$, given in μ_N, is the matrix element of the allowed operator, neglecting the tensor correction. The absolute value of the experimental matrix elements $|M1|$ are taken from this work or ENSDF [31–33] with assumed ground-state spin $J_{\rm gs}$. The (+) and (−) values for g_p reflect the uncertainty of the sign of the experimental matrix elements.

	S_π	S_ν	L_π	L_ν	P_π	P_ν	$M1_{L+S}$	$J_{\rm gs}$	$\lvert M1\rvert_{\rm exp}$	$g_p(+)$	$g_p(-)$
^{37}Cl	0.051	0.000	−0.051	0.000	0.400	0.000	0.157	3/2	0.33(4)	0.44(10)	−1.22(10)
^{39}K	0.000	0.000	0.000	0.000	0.535	0.000	0.000	3/2	0.22(2)	0.42(3)	−0.42(3)
^{45}Cl	0.058	0.007	−0.138	0.073	0.469	0.001	0.064	1/2	0.47(3)	0.86(6)	−1.14(6)
^{45}Cl								3/2	0.33(2)	0.57(5)	−0.85(5)
^{47}K	0.020	−0.007	−0.142	0.128	0.540	0.002	−0.063	1/2	0.055(8)	0.22(1)	0.01(1)

substantial underestimation of the calculated $M1$ transition strength between the first excited state and the ground state. Using the free-nucleon $M1$ operator, SDPF-U predicts $B(M1\downarrow) = 0.0063\mu_N^2$, while the use of the effective $M1$ operator of Ref. [16] ($g_s = 0.75 g_s^{\rm free}$, $g_\ell^\pi = 1.1$, $g_\ell^\nu = -0.1$) yields $B(M1\downarrow) = 0.0010\mu_N^2$, both an order of magnitude below the measured value. EPQQM produces a value three orders of magnitude smaller than that of SDPF-U, so for the remaining discussion of $M1$ strength we will focus on SDPF-U. In the SDPF-U calculation, the ground state is dominated by proton $(s_{1/2})^1$ configurations (80%), while the first excited state consists of only 26% $(s_{1/2})^1$, leading to an ℓ-forbidden ($\Delta\ell = 2$) transition.

ℓ-Forbidden $M1$ transitions are particularly sensitive to a tensor correction to the effective $M1$ operator of the form [28]

$$\delta(M1) = g_P\sqrt{8\pi}\left[\mathbf{Y}^{(2)}\otimes\mathbf{S}\right]^{\Delta J=1}, \qquad (1)$$

where g_P is the tensor effective g factor, $\mathbf{Y}^{(2)}$ is a rank-2 spherical harmonic, and $\mathbf{S}$ is the spin operator (see also Ref. [29] for pioneering experimental work). Because the g_s and g_ℓ values in Ref. [16] reproduce several magnetic moments in neutron-rich nuclei around $N = 28$, we leave the allowed part of the $M1$ operator unchanged and deduce the tensor g-factor g_P required to reproduce the experimental $M1$ transition strength.

Table III shows the results for four ℓ-forbidden transitions. It is apparent that, especially in ^{45}Cl, the spin and orbital contributions are small and add destructively, resulting in an $M1$ strength dominated by the proton tensor component.

The $N = 20$ nuclei, ^{37}Cl and ^{39}K, both require a tensor g factor of around 0.4, in agreement with an empirical fit for the sd shell [28], while the g factors required for the $N = 28$ nuclei differ significantly. One possible source of this discrepancy is that the cross-shell proton-neutron matrix elements, which do not affect the $N = 20$ nuclei, do not accurately predict the configuration mixing in the low lying states of the $N = 28$ nuclei. These matrix elements, and in particular the off-diagonal elements, are currently not well constrained by data. In order to estimate the uncertainty in the $M1$ due to this part of the Hamiltonian, we have replaced the cross-shell portion of SDPF-U with a realistic interaction derived from an N^{3}LO (fourth-order chiral perturbation theory) nucleon-nucleon potential [23] as described in Ref. [24]. We obtain an effective low-momentum interaction [25] with a cutoff of $\Lambda = 2.2\,{\rm fm}^{-1}$, and renormalize to the sd-pf model space using Rayleigh-Schrödinger perturbation theory to second order [26], including excitations up to $4\hbar\omega$ relative to a ^{42}Si core with harmonic oscillator wave functions and single-particle energies. To better reproduce level schemes in the region, the monopole cross-shell terms were adjusted to be

$$\langle ab|V|ab\rangle_J = \langle ab|V_{\rm U}|ab\rangle_J + \overline{V}_{N3LO}(ab) - \overline{V}_{\rm U}(ab),$$

where $V_{\rm U}$ is the SDPF-U interaction and $\overline{V}$ indicates a $2J+1$-weighted average over J. The results are shown in Table IV.

The experimental $M1$ value for ^{47}K can now be well reproduced with the same effective operator as the sd-shell nuclei, indicating that the theoretical value is sensitive to the off-diagonal cross-shell terms. For ^{45}Cl, the change is less significant and the tensor correction required is still more than double that of the other nuclei considered. However, the ground-state J^π assignment of ^{45}Cl has not been established experimentally, although $1/2^+$ has been favored from systematics and comparisons with theory [8,27]. Given that the ground and first excited state are within less than 200 keV, a $3/2^+$ ground-state and $1/2^+$ excited-state assignment has to be considered. Indeed, assuming that the ^{45}Cl ground state is $J^\pi = 3/2^+$ and the first excited state is $J^\pi = 1/2^+$ brings the required tensor correction significantly closer to that of the other ℓ-forbidden transitions. This makes the

TABLE IV. Results of a calculation using SDPF-U with a modified cross-shell interaction (see text). The results for the $N = 20$ nuclei are unchanged by the modification.

	S_π	S_ν	L_π	L_ν	P_π	P_ν	$M1_{L+S}$	$J_{\rm gs}$	$\lvert M1\rvert_{\rm exp}$	$g_p(+)$	$g_p(-)$
^{45}Cl	0.058	0.024	−0.087	0.006	0.405	0.006	0.076	1/2	0.47(3)	0.97(7)	−1.34(7)
^{45}Cl								3/2	0.33(2)	0.63(5)	−1.01(5)
^{47}K	0.024	0.011	−0.192	0.157	0.535	−0.003	−0.160	1/2	0.055(8)	0.40(1)	0.20(1)

TABLE V. $B(E2; J_i \rightarrow J_f)$ values for ^{45}Cl calculated using SDPF-U and standard effective charges of $e_p = 1.5$ and $e_n = 0.5$.

	$B(E2\uparrow)$
$1/2^+_1 \rightarrow 3/2^+_2$	203
$1/2^+_1 \rightarrow 5/2^+_1$	203
$3/2^+_1 \rightarrow 3/2^+_2$	111
$3/2^+_1 \rightarrow 5/2^+_1$	194
Ibbotson *et al.*	87(24)

firm determination of the ^{45}Cl ground-state spin an important experimental challenge.

It is interesting to compare other measured transition strengths to the shell-model calculations. Ibbotson *et al.* studied ^{45}Cl in intermediate-energy Coulomb excitation and observed a state at 929(17) keV. With the assumption of pure $E2$ character, a $B(E2\uparrow)$ value of $87(24)e^2\text{fm}^4$ was deduced from the measured Coulomb excitation cross section [14]. A peak around 765 keV, roughly half as intense as the 929 kev peak, may also be present in the spectrum, although its strength is not evaluated as the peak is partly obscured by the 548 keV peak from the ^{197}Au target. The corresponding shell-model calculations with the SDPF-U interaction are shown in Table V. Regardless of the choice of ground-state spin, the calculation significantly overpredicts the low-lying quadrupole collectivity, consistent with a recent study of ^{47}Ar [30]. It thus appears that SDPF-U underpredicts configuration mixing leading to allowed $M1$ transitions, while at the same time overpredicting quadrupole collectivity.

C. ^{44}Cl and ^{46}Cl

γ-Ray spectra in coincidence with ^{44}Cl and ^{46}Cl are shown in Fig. 9. The ^{44}Cl transitions at 475, 518, and 725 keV were reported previously in Ref. [15], while the other transitions at 107, 351, 892, and 997 keV were not known before (Table VI). Additionally, small peaks at 610, 631, 1091, 1151, and 1226 keV are seen. The large width of the peak at 475 keV was attributed in Ref. [15] to a lifetime effect ($\tau = 1.5^{+5.0}_{-0.5}$ ns). However, in our less-selective reaction, it is possible that several weak transitions from the predicted, closely spaced multiplet of states around 500 keV are superimposed on that peak structure. Shell model calculations with the SDPF-U interaction predict five quasidegenerate states around 500 keV, while the EPQQM interaction predicts three quasidegenerate states in that region (Fig. 10). No $\gamma\gamma$ coincidences were observed for ^{44}Cl.

TABLE VI. γ-Rays, efficiency-corrected relative intensities, and coincidences for ^{44}Cl.

E_γ [keV]	I_γ [%]	Coincident γ-rays
107	5(1)	
475	36(5)	
518	100(3)	
725	76(3)	
892	29(3)	
996	14(2)	

In comparison to SDPF-NR shell-model calculations, Riley *et al.* attribute the 475 keV transition to the de-excitation of the 4^-_1 state to the 2^- ground state based on the $E2$ transition strength deduced from the lifetime estimate. The ground-state g factor measurement by De Rydt *et al.* [16] strongly supports the assignment of 2^- for the ground state of ^{44}Cl. The EPQQM effective interaction predicts a very different level scheme with a 0^- ground state and the first 2^- and 4^- states around 500 keV. Firm spin assignments from experiment are needed for these odd-odd nuclei to discriminate between the two very different shell-model results. The widely different calculated excitation spectra underline the potential of odd-odd nuclei to provide extremely sensitive benchmarks for theory.

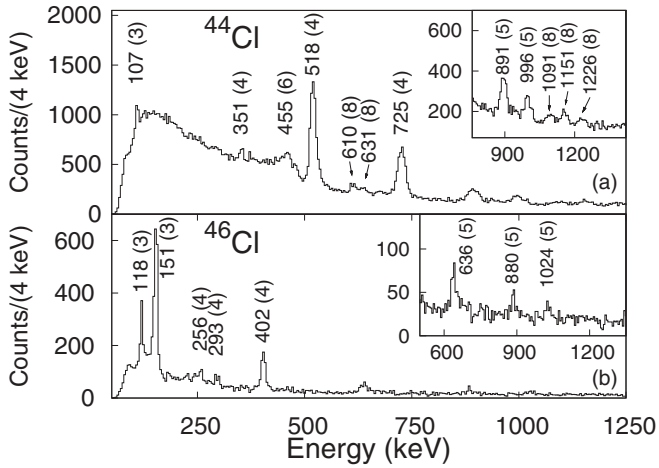

FIG. 9. Doppler-corrected γ-ray spectra detected in coincidence with ^{44}Cl (top figure, $v/c = 0.0.395$) and ^{46}Cl (bottom figure, $v/c = 0.385$). The insets show the spectra expanded in the region of the weaker transitions.

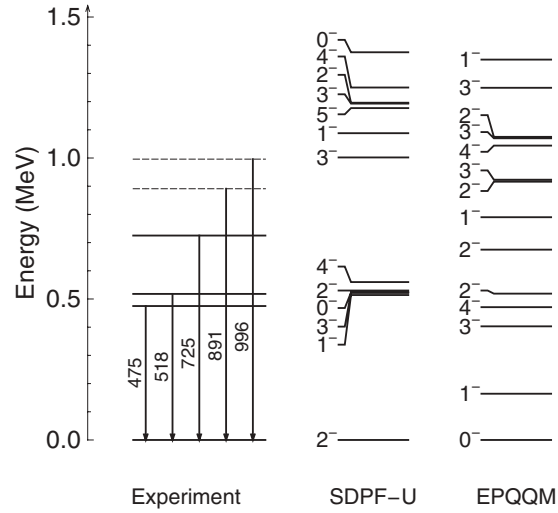

FIG. 10. Level schemes for ^{44}Cl from this work and shell-model calculations using SDPF-U and EPQQM effective interactions. The dashed lines in the experimental level scheme indicate tentative level assignments.

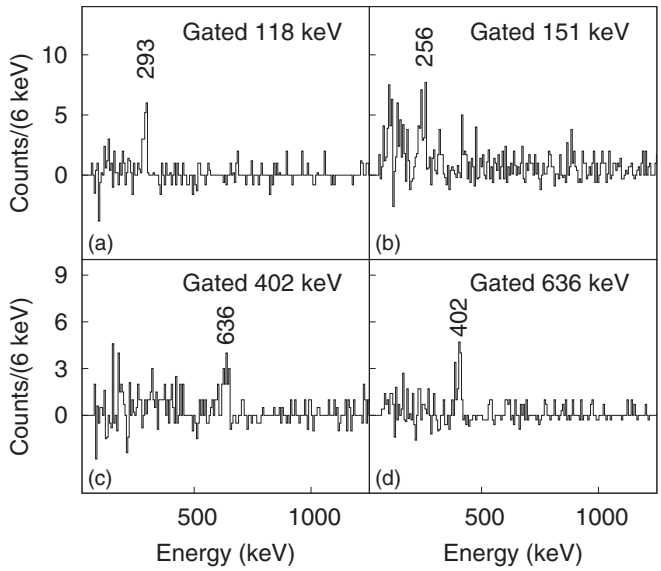

FIG. 11. Background-subtracted $\gamma\gamma$ coincidence spectra for ^{46}Cl.

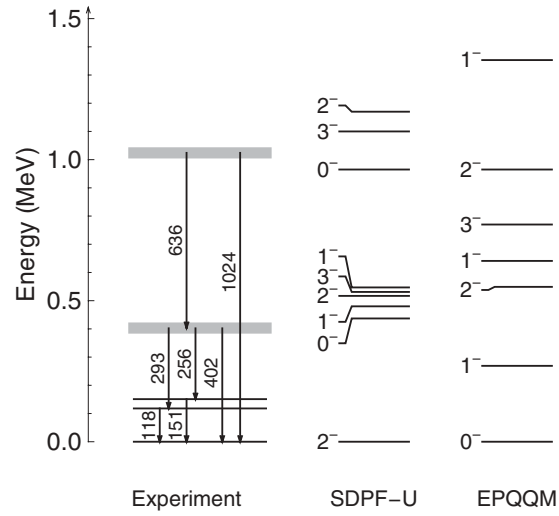

FIG. 12. Level scheme for ^{46}Cl from this work and shell-model calculations using SPDF-U and EPQQM effective interactions. The shaded gray bars in the experimental level scheme indicate a possible unresolved multiplet of states.

Eight transitions are observed in coincidence with ^{46}Cl for the first time, and several $\gamma\gamma$ coincidences are seen (Fig. 11 and Table VII). The sum of the coincident 151- and 256-keV γ rays [407(5) keV], the sum of the coincident 118- and 293-keV γ rays [411(5) keV], and the 402(4)-keV transition all agree with 406 keV within uncertainty. The coincident 402- and 636-keV transitions sum to 1038(6) keV, which just misses coinciding with the 1024(5) keV transition within uncertainty. In both cases, it is unclear whether there is one level, or multiple closely spaced levels. From this information, we construct the level scheme presented in Fig. 12, where the ordering of states is based on intensity balances and the shaded gray bars indicate a possible unresolved multiplet of states. While clusters of states around 500 and 1000 keV are reproduced reasonably well by the SDPF-U calculation, the two low-lying states below 200 keV are not. As in ^{44}Cl, the EPQQM calculation produces a drastically different level scheme with a 0^- ground state, in contrast to the 2^- ground state predicted by SDPF-U. Again, firm experimental spin assignments are needed to guide the widely varying shell-model calculations for this odd-odd system.

TABLE VII. γ-Rays, efficiency-corrected relative intensities, and coincidences for ^{46}Cl.

E_γ [keV]	I_γ [%]	Coincident γ rays
118	29(3)	293
151	100(4)	256
256	11(2)	151
293	8(2)	118
402	51(4)	636
636	29(4)	402
880	13(3)	
1024	11(4)	

IV. SUMMARY

We report the in-beam γ-ray spectroscopy of neutron-rich chlorine isotopes populated by fragmentation of a ^{48}K projectile beam on a thick Be target. One new transition in ^{43}Cl, nine in ^{44}Cl, six in ^{45}Cl, and eight new transitions in ^{46}Cl—for which no previous spectroscopic data was available before—were observed. $\gamma\gamma$ coincidences were used to generate experimental level schemes up to 2 MeV for ^{43}Cl, ^{45}Cl, and ^{46}Cl, although no firm spin assignments could be made from our measurement. The level schemes are compared to large-scale shell-model calculations with the SDPF-U and EPQQM effective interactions, showing best agreement with the SDPF-U for the even-N nuclei. For the odd-odd nuclei ^{44,46}Cl, the two shell-model effective interactions differ widely and firm spin assignments are needed to guide theory. The lifetime of the first excited state in ^{45}Cl was obtained through a γ-ray line-shape analysis, yielding an $M1$ transition strength that is significantly underpredicted by the shell-model calculations. This observation is discussed in the framework of tensor corrections to the effective $M1$ operator for ℓ-forbidden transitions. The $M1$ strength reported here hints at the possibility that—contrary to theory and systematics—the ground state of ^{45}Cl may have $J^\pi = 3/2^+$. These measurements underline the potential of odd-mass and odd-odd nuclei to sensitively and systematically benchmark shell-model calculations.

ACKNOWLEDGMENTS

This material is based upon work supported by the Department of Energy National Nuclear Security Administration under Award No. DE-NA0000979. This work was also supported by the National Science Foundation under Grants No. PHY-0606007, No. PHY-1102511, and No. PHY-1068217. A.G. is supported by the Alfred P. Sloan Foundation.

[1] B. A. Brown, Prog. Part. Nucl. Phys. **47**, 517 (2001).
[2] O. Sorlin and M.-G. Porquet, Prog. Part. Nucl. Phys. **61**, 602 (2008).
[3] A. Gade and T. Glasmacher, Prog. Part. Nucl. Phys. **60**, 161 (2008).
[4] T. Glasmacher *et al*., Phys. Lett. B **395**, 163 (1997).
[5] B. Bastin *et al*., Phys. Rev. Lett. **99**, 022503 (2007).
[6] C. Force *et al*., Phys. Rev. Lett. **105**, 102501 (2010).
[7] D. Santiago-Gonzalez *et al*., Phys. Rev. C **83**, 061305(R) (2011).
[8] A. Gade *et al*., Phys. Rev. C **74**, 034322 (2006).
[9] J. Fridmann *et al*., Phys. Rev. C **74**, 034313 (2006).
[10] T. Otsuka, T. Suzuki, R. Fujimoto, H. Grawe, and Y. Akaishi, Phys. Rev. Lett. **95**, 232502 (2005).
[11] F. Nowacki and A. Poves, Phys. Rev. C **79**, 014310 (2009).
[12] K. Kaneko, Y. Sun, T. Mizusaki, and M. Hasegawa, Phys. Rev. C **83**, 014320 (2011).
[13] O. Sorlin *et al*., Eur. Phys. J. A **22**, 173 (2004).
[14] R. W. Ibbotson, T. Glasmacher, P. F. Mantica, and H. Scheit, Phys. Rev. C **59**, 642 (1999).
[15] L. A. Riley *et al*., Phys. Rev. C **79**, 051303(R) (2009).
[16] M. De Rydt *et al*., Phys. Rev. C **81**, 034308 (2010).
[17] A. Gade *et al*., Phys. Rev. Lett. **102**, 182502 (2009).
[18] D. J. Morrissey, B. M. Sherrill, M. Steiner, A. Stolz, and I. Wiedenhoever, Nucl. Instrum. Methods Phys. Res. B **204**, 90 (2003).
[19] D. Bazin, J. A. Caggiano, B. M. Sherrill, J. Yurkon, and A. Zeller, Nucl. Instrum. Methods in Phys. Res. B **204**, 629 (2003).
[20] W. F. Mueller, J. A. Church, T. Glasmacher, D. Gutknecht, G. Hackman, P. G. Hansen, Z. Ju, K. L. Miller, and P. Quirin, Nucl. Instrum. Methods Phys. Res. A **466**, 492 (2001).
[21] S. Nummela *et al*., Phys. Rev. C **63**, 044316 (2001).
[22] S. Agostinelli *et al*., (Geant4 Collaboration), Nucl. Instr. Methods Phys. Res. A **506**, 250 (2003).
[23] D. R. Entem and R. Machleidt, Phys. Rev. C **68**, 041001(R) (2003).
[24] A. Signoracci, B. A. Brown, and M. Hjorth-Jensen, Phys. Rev. C **83**, 024315 (2011).
[25] S. K. Bogner, T. T. S. Kuo, and A. Schwenk, Phys. Rep. **386**, 1 (2003).
[26] M. Hjorth-Jensen, T. T. S. Kuo, and E. Osnes, Phys. Rep. **261**, 125 (1995).
[27] L. Caceres *et al*., Phys. Rev. C **85**, 024311 (2012).
[28] B. A. Brown and B. H. Wildenthal, Nucl. Phys. A **474**, 290 (1987).
[29] B. Reitz, F. Hofmann, P. von Neumann-Cosel, F. Neumeyer, C. Rangacharyulu, A. Richter, G. Schrieder, D. I. Sober, and B. A. Brown, Phys. Rev. Lett. **82**, 291 (1999).
[30] R. Winkler *et al*., Phys. Rev. Lett. **108**, 182501 (2012).
[31] J. Cameron, J. Chen, B. Singh, and N. Nica, Nucl. Data Sheets **113**, 365 (2012).
[32] J. Cameron and B. Singh, Nucl. Data Sheets **117**, 225 (2006).
[33] T. W. Burrows, Nucl. Data Sheets **108**, 923 (2007).